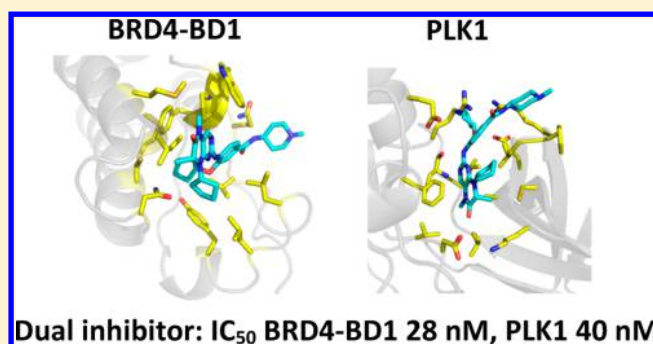


## Structure-Guided Design and Development of Potent and Selective Dual Bromodomain 4 (BRD4)/Polo-like Kinase 1 (PLK1) Inhibitors

Shuai Liu,<sup>†</sup> Hailemichael O. Yosief,<sup>†</sup> Lingling Dai,<sup>‡,||</sup> He Huang,<sup>⊥</sup> Gagan Dhawan,<sup>†,‡</sup> Xiaofeng Zhang,<sup>†</sup> Alex M. Muthengi,<sup>†</sup> Justin Roberts,<sup>§</sup> Dennis L. Buckley,<sup>§</sup> Jennifer A. Perry,<sup>‡</sup> Lei Wu,<sup>‡</sup> James E. Bradner,<sup>\*,§,▽,||</sup> Jun Qi,<sup>\*,‡,||</sup> and Wei Zhang<sup>\*,†,||</sup><sup>†</sup>Department of Chemistry, University of Massachusetts—Boston, Boston, Massachusetts 02125, United States<sup>‡</sup>Department of Cancer Biology and <sup>§</sup>Department of Medical Oncology, Dana-Farber Cancer Institute, Boston, Massachusetts 02215, United States<sup>||</sup>Phase I Clinical Trial Center & Department of Clinical Pharmacology, Xiangya Hospital, Central South University, Changsha, Hunan 410008, P.R. China<sup>⊥</sup>Department of Chemistry, Stony Brook University, Stony Brook, New York 11794-3400, United States<sup>#</sup>Department of Biomedical Science, Acharya Narendra Dev College, University of Delhi, New Delhi 110019, India<sup>▽</sup>Novartis Institutes for Biomedical Research, Cambridge, Massachusetts 02139, United States<sup>||</sup>Department of Medicine, Harvard Medical School, Boston, Massachusetts 02115, United States

## Supporting Information

**ABSTRACT:** The simultaneous inhibition of polo-like kinase 1 (PLK1) and BRD4 bromodomain by a single molecule could lead to the development of an effective therapeutic strategy for a variety of diseases in which PLK1 and BRD4 are implicated. Compound 23 has been found to be a potent dual kinase–bromodomain inhibitor (BRD4-BD1 IC<sub>50</sub> = 28 nM, PLK1 IC<sub>50</sub> = 40 nM). Compound 6 was found to be the most selective PLK1 inhibitor over BRD4 in our series (BRD4-BD1 IC<sub>50</sub> = 2579 nM, PLK1 IC<sub>50</sub> = 9.9 nM). Molecular docking studies with 23 and BRD4-BD1/PLK1 as well as with 6 corroborate the biochemical assay results.



## INTRODUCTION

The bromodomain and extra-terminal domain (BET) family of proteins is essential for recognizing acetylated lysines (KAc) on chromatin and has emerged as a potential therapeutic target for the treatment of cancer, inflammation, and viral infectious diseases.<sup>1–8</sup> BET proteins, including BRD2, BRD3, BRD4, and BRDT, are characterized by dual bromodomains (BD1 and BD2) that bind to KAc on histones to facilitate the recruitment and stabilization of protein complexes, which plays an active role in gene expression.<sup>9–13</sup> With the development of the first small molecule inhibitor of BET bromodomains, (+)-JQ1, we were able to demonstrate that binding to BRD4 displaces BRD4 from chromatin and interrupts the biological function of the protein.<sup>3,14</sup> Since our initial reports, several potent and selective BET inhibitors with different chemotypes have been reported to possess binding affinities, selectivity profiles, and cellular activities that are similar to those of (+)-JQ1.<sup>15–19</sup> More importantly, more than 12 BET bromodomain inhibitors have progressed into clinical trials, including a derivative of JQ1,<sup>20</sup> for the treatment of hematologic malignancies, solid tumors, and cardiovascular disease.<sup>21</sup> With multiple cancer studies demonstrating the development of resistance to single

agents, including BET inhibitors, strategies for combination therapies are being intently pursued.<sup>22–24</sup>

Recent reports highlight that the inhibition of polo-like kinase 1 (PLK1), a crucial cell-cycle regulator, synergizes with BET inhibition in multiple cancer types, including prostate cancer and acute myeloid leukemia (AML).<sup>25,26</sup> While combinatorial inhibition of PLK1 and BET bromodomains with two molecules appears to be synergistic,<sup>26</sup> achieving this with a single agent may increase potency for two disease-relevant targets/pathways while decreasing toxicity. The concept has recently been demonstrated with dual PI3K-BRD4 inhibitors that have recently been reported to block the expression of the MYC oncogene, while markedly inhibiting cancer cell growth and metastasis in hepatocellular carcinoma and neuroblastoma in vivo.<sup>27,28</sup> The recent discovery that multiple kinase inhibitors, including the PLK1 inhibitor, BI-2536, and the janus kinase 2 (JAK2) inhibitor, TG101209, (Figure 1) exhibit moderate to excellent inhibitory activity against the BET family of proteins opens up the possibility of

Received: May 14, 2018

Published: August 20, 2018

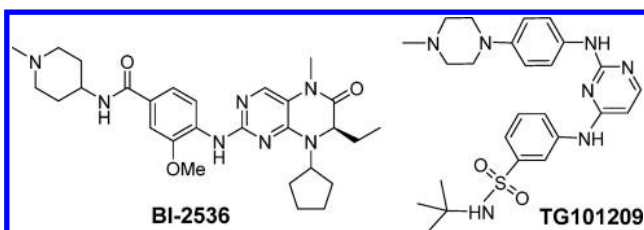


**Figure 1.** Kinase inhibitors with nanomolar inhibitory activity against BRD4.

creating polypharmacological compounds that target both kinases and BET proteins equivalently.<sup>7,23,29–32</sup>

In this study, we utilized the scaffold of BI-2536 to develop inhibitors with varied inhibitory activities against BRD4 and PLK1 in order to perform structure–activity relationship (SAR) studies, as well as understand the effect of inhibiting both proteins (PLK1 and BRD4) with a single agent in cancer, as both the BET family of proteins and PLK1 are intently pursued targets for the treatment of cancer.

First, we inspected the binding modes of BI-2536 with BRD4-BD1 and PLK1, respectively, through cocrystallization studies (Figure 2). In the binding complex of BI-2536 with BRD4-BD1, the methylated amide functions as an acetylated lysine mimic, where the carbonyl oxygen of the dihydropteridinone ring forms a water-mediated hydrogen bond with the conserved acetyl lysine recognition motif, asparagine (N140), in the binding pocket. The methyl group is orientated into a hydrophobic subpocket formed by F83, I146, and C136. The NH group on the aniline and one of the pyrimidine nitrogen atoms interact with the Q85 backbone amide through an intermediary water molecule. The ethyl group that branches off of the asymmetric dihydropteridinone carbon atom is projected into a small hydrophobic subpocket formed by V87, L92, L94, and Y97, while the cyclopentyl moiety and the *N*-methylpiperidine are both solvent exposed.<sup>29,30</sup>

On the basis of structural information from the cocrystals, we envisioned several strategies to improve the BRD4-BD1 binding affinity while reducing the PLK1 inhibition to achieve

balanced dual PLK1/BRD4-BD1 inhibition (Figure 3). First, we hypothesize that the replacement of the amide methyl group at site 1 with a slightly larger ethyl or isopropyl might enhance binding affinity to BRD4-BD1. Second, to decrease the affinity for PLK1, the elaboration of the 3-methoxy group on the aromatic ring (site 2) with a bulkier group might modulate binding affinity. This methyl ether group is involved in critical hydrogen bonds with the PLK1 active site (Figure 2B). The interruption of this interaction is expected to reduce the PLK1 binding affinity of BI-2536 but render its activity to BRD4-BD1 unchanged. Third, modification on the ethyl group might have more impact on PLK1 activity as the pocket in PLK1 is narrower compared to the binding pocket in BRD4-BD1. In the end, we will modify the solvent exposed sites (sites 4 and 5) to fully investigate the effect of each group on the binding affinity of the parent compound toward BRD4-BD1 and PLK1 based on the chemistry we established previously developing fluorescently tagged kinase inhibitors.<sup>31</sup> Thus, we conducted a medicinal chemistry campaign around the BI-2536 core to develop small molecules with fine-tuned activities against PLK1 and BET bromodomains.

## RESULTS AND DISCUSSION

Utilizing the structural information from the cocrystal structures of BI-2536 with BRD4-BD1 and PLK1, a series of BI-2536 analogues were synthesized using the general synthesis route shown in Scheme 1. In brief, amino acids with varying alkyl side chains (different R<sup>1</sup> group) were esterified with thionyl chloride in MeOH followed by alkylation using reductive amination with cyclic or acyclic ketones. The resulting secondary amine derivative, E1, underwent a regioselective nucleophilic aromatic substitution reaction with 2,6-dichloro-5-nitropyrimidine to produce tertiary anilines. The nitro group was reduced using zinc dust in hot acetic acid, generating the dihydropteridinone ring in E2. Methylation of the amide produced scaffold E3, which was used in a nucleophilic substitution reaction with the aminobenzoic acid derivative and led to the formation of intermediate E4 with an acid motif, which was coupled with different amines to

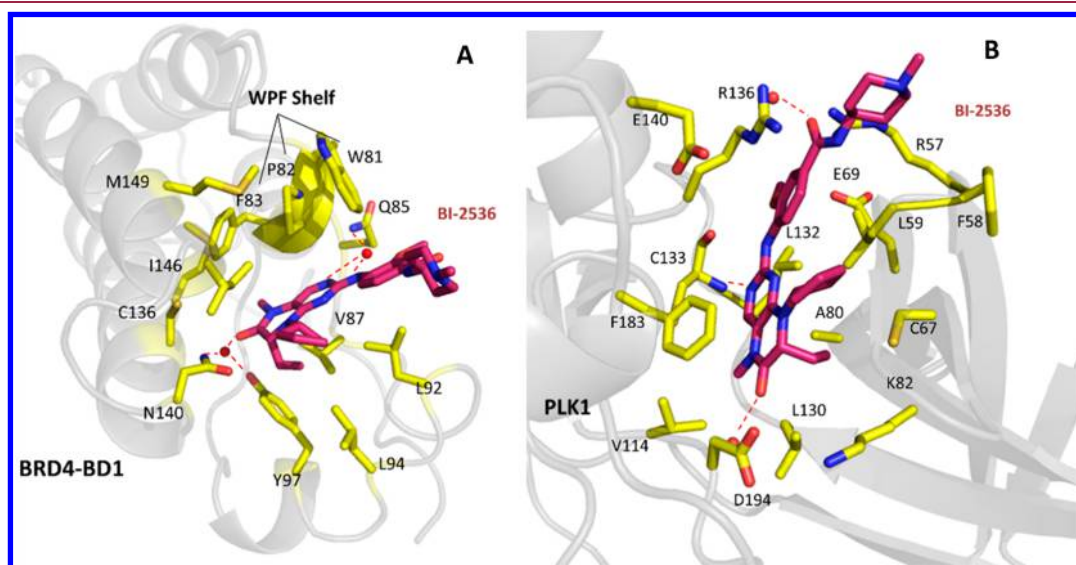


**Figure 2.** Crystal structure of BI-2536 (dark red) bound to (A) BRD4-BD1 (PDB ID: 4O74) and (B) PLK1 (PDB ID: 2RKU). The protein residues in contact with the ligand are represented by yellow sticks; hydrogen bonding is represented by red dashed lines, and the remaining residues near the binding pocket are shown in gray.

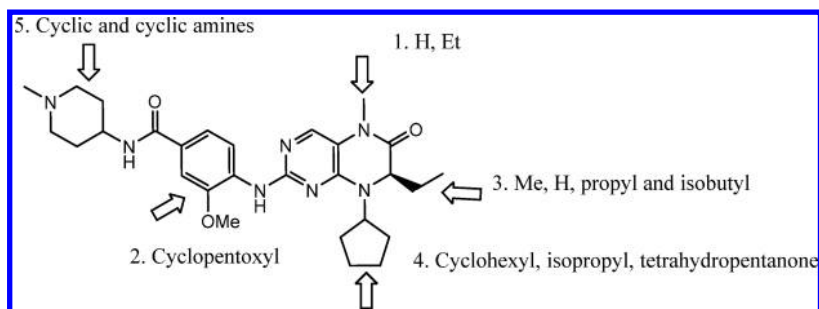


Figure 3. Available modification sites on BI-2536.

Scheme 1. Synthesis of BI-2536 Analogues 1–20

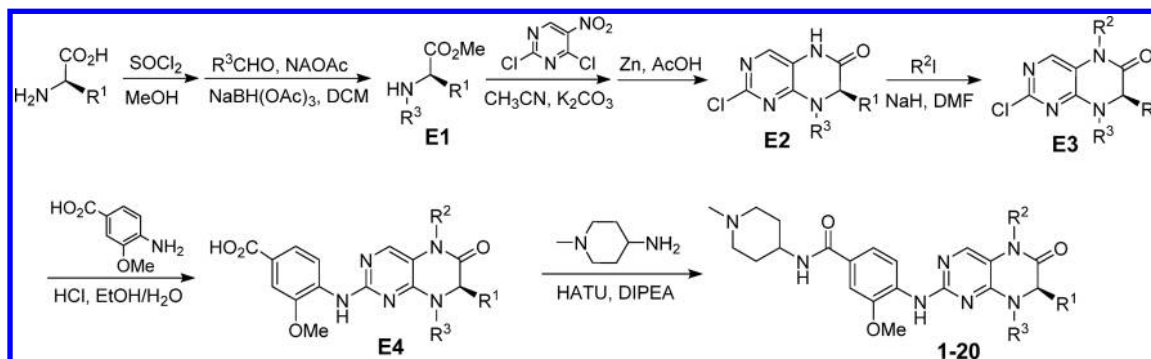
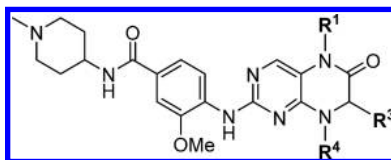


Table 1. Structure–Activity Relationships on BI-2536 Analogues



compound	R <sup>4</sup>	R <sup>3</sup>	R <sup>1</sup>	IC <sub>50</sub> (μM)		
				BRD4-BD1 <sup>a</sup>	PLK1 <sup>b</sup>	BRDT-BD1 <sup>a</sup>
BI-2536	Cp	(R)-Et	Me	0.205 ± 0.008	0.004	ND <sup>c</sup>
1	Cy	(R)-Et	Me	0.65 ± 0.024	0.004	ND
2	<i>i</i> -Pr	(R)-Et	Me	0.186 ± 0.013	0.004	ND
3	<i>i</i> -Pr	(R)-Et	H	>10	2.62	ND
4	Cy	(R)-Et	H	>10	0.0372	ND
5	Cp	(R)-Me	Me	0.084 ± 0.006	0.0011	0.342 ± 0.015
6	Cp	(R)-Pr	Me	2.579 ± 0.180	0.0099	8.468 ± 0.076
7	Cp	H	Me	6.633 ± 0.530	0.0541	25.99 ± 9.70
8	Cp	(R)- <i>i</i> Bu	Me	18.8 ± 3.4	0.078	ND
9	Cp	(S)-Me	Me	0.107 ± 0.002	0.0087	0.229 ± 0.010
10	Cp	(S)-Et	Me	0.489 ± 0.017	0.0325	3.513 ± 0.351
11	Cy	(R)-Me	Me	0.31 ± 0.01	0.0086	0.75 ± 0.03
12	<i>i</i> -Pr	(R)-Me	Me	0.421 ± 0.016	0.0252	0.978 ± 0.043
13	tetrahydro-2H-pyran	(R)- <i>i</i> Bu	Me	>50	0.322	>50
14	<i>i</i> -Pr	(R)- <i>i</i> Bu	Me	41.9	0.218	ND
(S)-JQ1				0.032 ± 0.001		0.103 ± 0.004

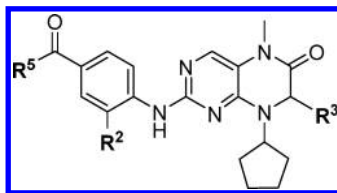
<sup>a</sup>IC<sub>50</sub> values were measured by an AlphaScreen binding assay and reported as the average of three replicates ± SE. <sup>b</sup>IC<sub>50</sub> values were measured using the Adapta assay format (ThermoFisher Scientific). <sup>c</sup>Not determined.

produce the final BI-2536 analogues. As planned in Figure 3, the resulting analogues include derivatives with different substituent groups on the amide bond (site 1); different ethers at site 2 with cyclic or acyclic motifs; varying substituent groups, such as hydrogen, methyl, propyl, and isobutyl on site 3; and the solvent-exposed site 4 or 5. All compounds in this focused library were then screened for their inhibitory activity

against BRD4-BD1 and BRDT-BD1 using AlphaScreen assay technology to obtain IC<sub>50</sub> values (all IC<sub>50</sub> values are for BD1 of all of the bromodomains tested unless otherwise noted).<sup>32</sup>

The modification of the cyclopentyl moiety at site 4 with different cyclic and acyclic groups, cyclohexyl (compound 1) and isopropyl (compound 2), created compounds with nanomolar inhibitory activity against BRD4 (Table 1). These

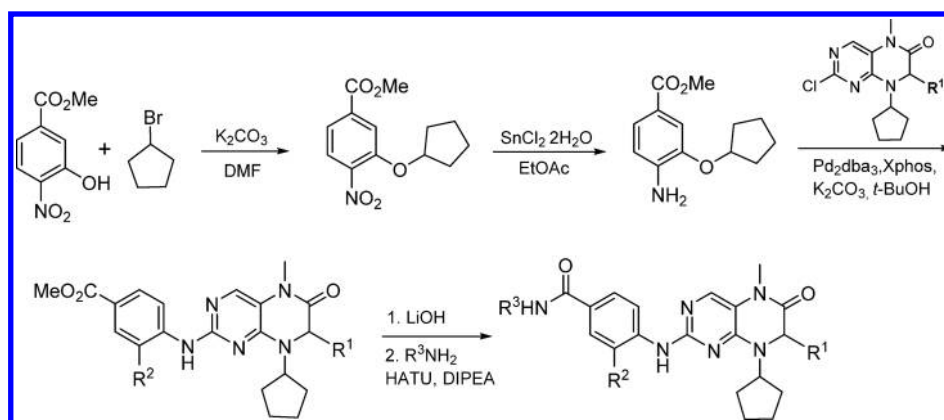
Table 2. Structure–Activity Relationship on Compound 5 Analogues



compound	R <sup>3</sup>	R <sup>2</sup>	R <sup>5</sup>	IC <sub>50</sub> (μM)		
				BRD4-BD1 <sup>a</sup>	PLK1 <sup>b</sup>	BRDT-BD1 <sup>a</sup>
5	(R)-Me	OMe	4-amine, 1-methylpiperidine	0.084 ± 0.006	0.0011	0.342 ± 0.015
15	(R)-Me	OMe	hexamethylene amine	0.107 ± 0.003	0.16	0.378 ± 0.014
16	(R)-Me	OMe	aminomethylpyridine	0.095 ± 0.002	0.0084	0.289 ± 0.008
17	(R)-Me	OMe	phenylethylamine	0.183 ± 0.009	0.027	0.558 ± 0.015
18	(R)-Me	OMe	<i>N,N</i> -dimethylethylamine	0.104 ± 0.050	0.021	0.392 ± 0.013
19	(R)-Me	OMe	aminopiperidine	0.109 ± 0.003	0.009	0.56 ± 0.025
20	(R)-Me	OMe	piperidine	0.094 ± 0.002	0.095	0.369 ± 0.011
21	(S)-Me	O-Cp	4-amine, 1-methylpiperidine	0.059 ± 0.001	0.127	0.245 ± 0.009
22	(R)-Me	O-Cp	OMe	0.253 ± 0.007	0.457	0.933 ± 0.032
23	(R)-Me	O-Cp	4-amine, 1-methylpiperidine	0.028 ± 0.001	0.04	0.102 ± 0.002
24	(R)-Pr	O-Cp	4-amine, 1-methylpiperidine	0.596 ± 0.014	0.047	1.951 ± 0.080
25	H	O-Cp	4-amine, 1-methylpiperidine	0.69 ± 0.018		3.543 ± 0.198

<sup>a</sup>IC<sub>50</sub> values were measured by an AlphaScreen binding assay and reported as the average of three replicates ± SE. <sup>b</sup>IC<sub>50</sub> values were measured using the Adapta assay format (ThermoFisher Scientific).

Scheme 2. Synthesis of 21 and 23–25



analogues, however, were less potent than parent compound BI-2536, indicating that the cyclopentyl group is crucial for the potent inhibitory activity against BRD4. These compounds, however, maintained low nanomolar inhibitory activity against PLK1, suggesting that modification at site 4 is tolerated for PLK1 binding. On the other hand, unmethylated amide derivatives of compounds 1 and 2 (compounds 3 and 4, respectively) resulted in a more than 1000-fold decrease in binding affinity for BRD4. Interestingly, the inhibitors with unmethylated amide, compounds 3 and 4, displayed a more than 250-fold selectivity for PLK1 over BRD4, indicating the importance of the methylated amide as an *N*-acetylated lysine mimic for BRD4 binding. Thus, it is critical to have a methylated amide at site 1 to serve as an *N*-acetylated lysine mimic for bromodomain inhibition. Taken together, the replacement of the cyclopentyl group at site 4 together with an unmethylated amide reduces the BRD4 activity of the inhibitors while maintaining PLK1 selectivity.

Next, we examined the modification of site 3 with methyl (compound 5), propyl (compound 6), hydrogen (compound 7), and isobutyl (compound 8) substituents. The analogue

with a methyl substitution at the asymmetric dihydropyridinone carbon atom, compound 5, exhibited good inhibitory activity against both BRD4 (IC<sub>50</sub> = 84 nM) and PLK1 (IC<sub>50</sub> = 11 nM). Selectivity profiling against 32 bromodomains (BROMOscan) and 468 kinases (KINOMEScan)<sup>33</sup> confirmed selective activity for the BET subfamily and PLK kinases (PLK1–3) at 1 μM through the profiling platform at DiscoverX. Specifically, a 1 μM solution of compound 5 exhibited selective activity against BRD4-BD1 (12% of control) and PLK kinases (0.3–0.5% of control) (Supporting Information, Figure 1). No significant difference in binding activity was observed for the (*S*) and (*R*) isomers of the methyl substituent, which is similar to the observation made on the (*S*) and (*R*) isomers of BI-2536 by the Fletcher group.<sup>32</sup> However, replacing the asymmetric ethyl group with bulky alkyl groups such as propyl (compound 6) and isobutyl (compound 8) groups resulted in a significant decrease in binding affinity toward BRD4. While compound 6 displayed excellent inhibitory activity against PLK1, with more than 250-fold selectivity over BRD4, further increasing the size of site 3

Table 3. Docking Results of Some BI-2536 Analogues on BRD4 and PLK1<sup>a</sup>

molecule	docking score (kcal/mol)		IC <sub>50</sub> (μM)		ligand–receptor interactions (vdw energy < −4 kcal/mol)	
	BRD4	PLK1	BRD4	PLK1	BRD4	PLK1
23	−7.34	−8.46	0.028	0.0400	Pro82, Gln85, Val87, Ile146	Leu59, Cys133, Arg136, Phe183
6	−6.54	−8.68	2.579	0.0099	Trp81, Pro82, Gln85, Val87, Leu92	Leu59, Arg136, Phe183
8	−6.63	−7.62	18.80	0.0780	Gln85, Val87, Asp88	Gly63, Asp194
5	−6.50	−8.23	0.084	0.0011	Val87, Asp88, Ile146	Leu59, Arg136, Phe183
BI-2536	−7.02	−8.60	0.025	0.00083	Leu92, Ile146	Arg57, Leu59, Arg136, Phe183

<sup>a</sup>Details in the Supporting Information.

with an isobutyl group or deleting the methyl group resulted in a reduction of PLK1 inhibitory activity.

With the improvement in BRD4 inhibitory activity with compound **5**, we further examined this compound through the replacement of the cyclopentyl group with cyclohexyl (compound **11**), tetrahydro-2H-pyran (compound **13**), and isopropyl (compound **12**) groups. None of these substitutions improved the potency toward BRD4 above that seen for compound **5**, further indicating that substituting the cyclopentyl moiety for the methyl group at the dihydropteridinone ring is optimal for BRD4 inhibition. On the other hand, the inhibitory activity of those analogues against PLK1 remained in the low nanomolar range. Similarly, replacing the cyclopentyl group of compound **8** with tetrahydro-2H-pyran (compound **13**) and isopropyl (compound **14**) groups did not improve the potency toward BRD4 but showed modest inhibitory activity against PLK1, suggesting that PLK1 is tolerant of substitutions at the asymmetric carbon and anilide nitrogen (Table 1). Taken together, the adjustment of substituent groups at site 3 tunes down BRD4 activity with little impact on PLK1 activity, leading us to discover the most PLK1 selective inhibitor in the series, compound **6** (>260-fold).

To increase the BRD4 selectivity of BI-2536 analogues, we utilized compound **5** to further explore the SAR around the terminal amine (site 5) and the methoxy group at site 2 to investigate their impact on potency and selectivity (Table 2 and the synthesis route shown in Scheme 2). Replacement of the terminal cyclic amine (amino-piperidine, site 5) with different alkyl and aromatic amines (compounds **15**–**20**) did not grossly impact the potency and selectivity for BRD4, implying that the various amine replacements are not engaged in any significant interaction with the amino acid residues in the binding pocket of BRD4. On the other hand, the modification of the methoxy moiety (site 2) with a cyclopentoxyl group improved the potency toward bromodomains while reducing the potency against PLK1. These substitutions created a molecule that has a relatively balanced potency toward both PLK1 and BRD4 with a less than 2-fold selectivity difference (Table 2). Notably, compound **23** exhibited improved potency for BRD4 compared to that of our reference BET inhibitor, (+)-JQ1, but reduced activity against PLK1 compared to that of BI-2536, making it one of the most potent BET bromodomain inhibitors with reduced PLK1 inhibition in the series. This improvement can be overridden by introducing a larger propyl group (compound **24**) at site 1. Also, the (*S*)-isomer of compound **23**, **21**, retains good inhibitory activity against BRD4 but is less potent toward PLK1, suggesting that the chirality change has more impact on PLK1 activity than on BRD4 activity, which is consistent with the SAR we established in the previous round. Finally, we examined the three compounds with the most balanced BRD4 and PLK1 activities (compounds **5**, **6**, and **23**) in a human

acute myeloid leukemia (AML) cell line, MOLM13. In general, BRD4 bromodomain inhibition causes a G1 arrest in the cell cycle as demonstrated by JQ1, while dual PLK1/BRD4 inhibitors, such as BI-2536, cause a G1/G2 arrest in the cell cycle. A 24 h treatment with compound **23** caused cell cycle arrest in the G1/G2 stage of the cell cycle, suggesting that it is functionally inhibiting both BRD4 and PLK1 (Supporting Information, Figure 2).

To gain a better understanding of the potency and predict the binding modes of our BI-2536 analogues, we utilized molecular modeling with PLK1 and BRD4-BD1 (Table 3). As described above, compound **23** shows equivalent potency for both BRD4 and PLK1, while compound **6** demonstrates the most selectivity for PLK1 over BRD4 in the series. To gain a better understanding of how compound **23** interacts with BRD4, we further modeled the docking of **23** with BRD4-BD1. As shown in Figure 4B, all of the interactions between residues on BRD4 and BI-2536 are conserved when **23** resides in the active site of BRD4. The conserved phenyl ring in the center of compound **23** develops  $\pi$ – $\pi$  stacking interactions with the aromatic rings in the WPF shelf (W81, P82, F83) of BRD4 as seen with the parental compound BI-2536. Furthermore, almost all of the original binding patterns established in our cocrystallography study of BI-2536 and BRD4 (Figure 2) are strengthened as indicated by the van der Waals (vdw) interaction energy decomposition, where stronger interactions formed with P82, Q85, V87, C136, N140, I146, and compound **23** (Figure 4A). Although the L92, L94, and Y97 hydrophobic subpocket of BRD4 is moved further from the dihydropteridinone, the deep pocket formed by F83, I146, and M149 made closer contact with the newly embedded cyclopentane to compensate or even gain back the hydrophobic interaction loss (Figure 4B). Overall, the docking analysis of compound **23** with BRD4 is consistent with the binding affinity defined in our biochemical assays.

In modeling the docking between compound **23** and PLK1, we found that the C133 backbone amide nitrogen of PLK1 conserves its hydrogen bonding to the nitrogen of dihydropteridinone in **23**, as indicated by unchanged dips at residue C133 from the vdw energy decomposition. The  $\pi$ – $\pi$  stacking interaction between F83 and the dihydropteridinone in **23** is also conserved (Figure 5A). The resulting docking pose of **23** with PLK1 retains interactions similar to those of BI-2536 with PLK1 (Figure 5B). In addition, the methyl group in **23**, which replaced the original ethyl group in BI-2536, does not reduce interactions with A80 and K82 significantly. However, a notable difference upon the substitution of cyclopentane for the methyl group in **23** is that the cyclopentane extends deeper into the hydrophobic subpocket between R57, F58, and L59 and creates an additional interaction with R136 and E140 that could further stabilize the overall binding.

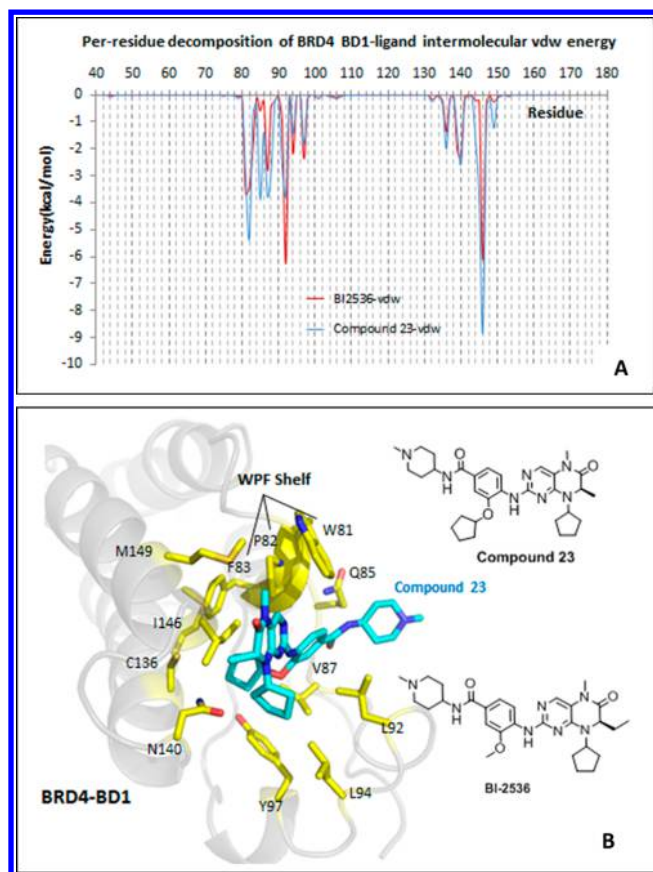


**Figure 4.** (A) Comparison of the per-residue decomposition of two BRD4-BD1 ligands, 23 in blue and BI-2536 in red, with intermolecular vdw interactions as a function of the receptor sequence. (B) Docking of 23 (cyan) with BRD4-BD1 (PDBID: 4O74); protein residues in contact with the ligand are represented by yellow sticks, and the rest are in gray.

Molecular modeling of compound 6 with BRD4-BD1 demonstrates that its docking pose demonstrates drastic variation from the cocrystal structure of BRD4-BD1 bound to BI-2536. When BI-2536 binds to BRD4-BD1, the dihydropteridinone and cyclopentane rings rest in between the WPF shelf (W81, P82, F83) and the BC loop (particularly N140 through the bridging water) of BRD4-BD1, with the ethyl group of BI-2536 pointing away to make additional contacts with V87, L92, L94, and Y97 (sharing the bridging water with N140) (Figure 6A,B). With BI-2536, Q85 interacts with the inhibitor through a water-mediated hydrogen bonding effect. However, the longer alkyl chain of compound 6 breaks this interaction due to steric clashes with L94 and Y97 (Figure 6C). Therefore, compound 6 has to adapt a novel orientation in the BRD4-BD1 active site, which demonstrates much weakened interactions by a striking positive vdw energy contribution from Y97. Although the phenyl ring of compound 6 shifts into the pocket thereby enhancing binding with the WPF shelf, it still cannot overcome the repulsive effect of the positive vdw effect. We believe that these adjustments contributed significantly toward the reduced activity of 6 against BRD4-BD1.

Alternatively, the molecular docking of compound 6 with PLK1 shows great similarity to BI-2536 cocrystallized with PLK1. The C133 residue is conserved and acts as a hydrogen bonding receptor to the nitrogen in the dihydropteridinone in

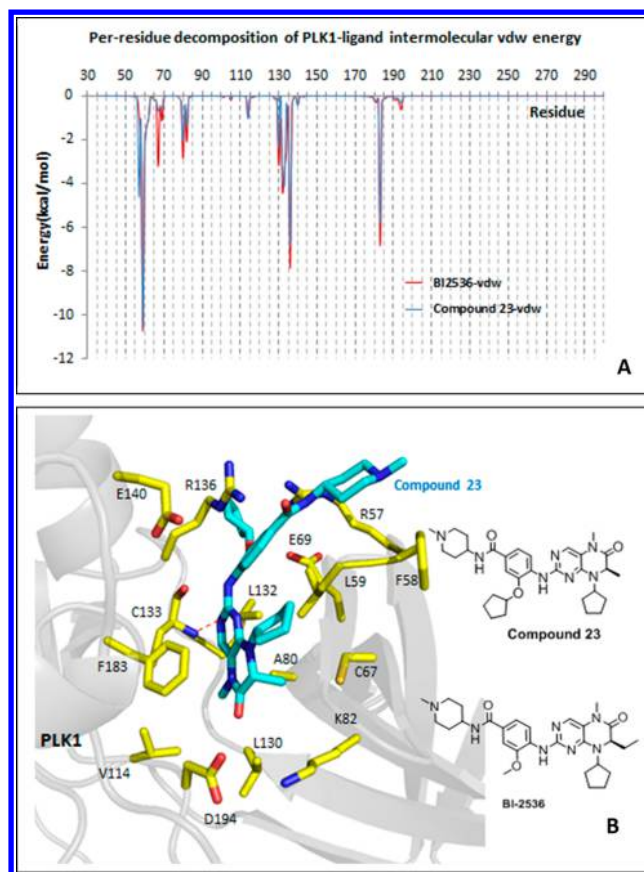


**Figure 5.** (A) Comparison of the per-residue decomposition of two PLK1 ligands, 23 in blue and BI-2536 in red, with intermolecular vdw interactions as a function of the receptor sequence. (B) Docking of 23 (cyan) in PLK1 (PDBID: 2RKU); protein residues in contact with the ligand are represented by yellow sticks, and the rest are in gray. Hydrogen bonding is represented by a red dashed line.

6, and the  $\pi$ - $\pi$  stacking interaction between F83 and the same aromatic ring is also kept (Figure 7A,B). Furthermore, the propyl group in 6, which replaced the original ethyl group in BI-2536 at site 3, does not reduce interactions with A80 and K82 much. The docking pose suggests that the carbonyl oxygen moved away from the active site but may form hydrogen bonds with either R136, R57, or crystal water, as was observed in the BI-2536-PLK1 complex structure, to reduce the entropy penalty when the new complex is forming. Again, the molecular docking analysis is in agreement with the binding affinity assays that illustrate a potent interaction between PLK1 and 6. The detailed ligand interaction diagrams (LID) are listed in the Supporting Information, Figures 3 and 4.

## CONCLUSIONS

Our focused SAR study of the dual kinase-bromodomain inhibitor, BI-2536, has led to the identification of potent, balanced inhibitors of BRD4 and PLK1, as well as a more PLK1 selective inhibitor. Through these studies, we determined the requirements for both PLK1 and BET protein binding. We determined that the methylated amide and the cyclopentyl group of the BI-2536 scaffold are important for maintaining bromodomain binding activity but less important for PLK1 inhibitory activity. Moreover, substituting the asymmetric ethyl moiety at the dihydropteridine ring with a

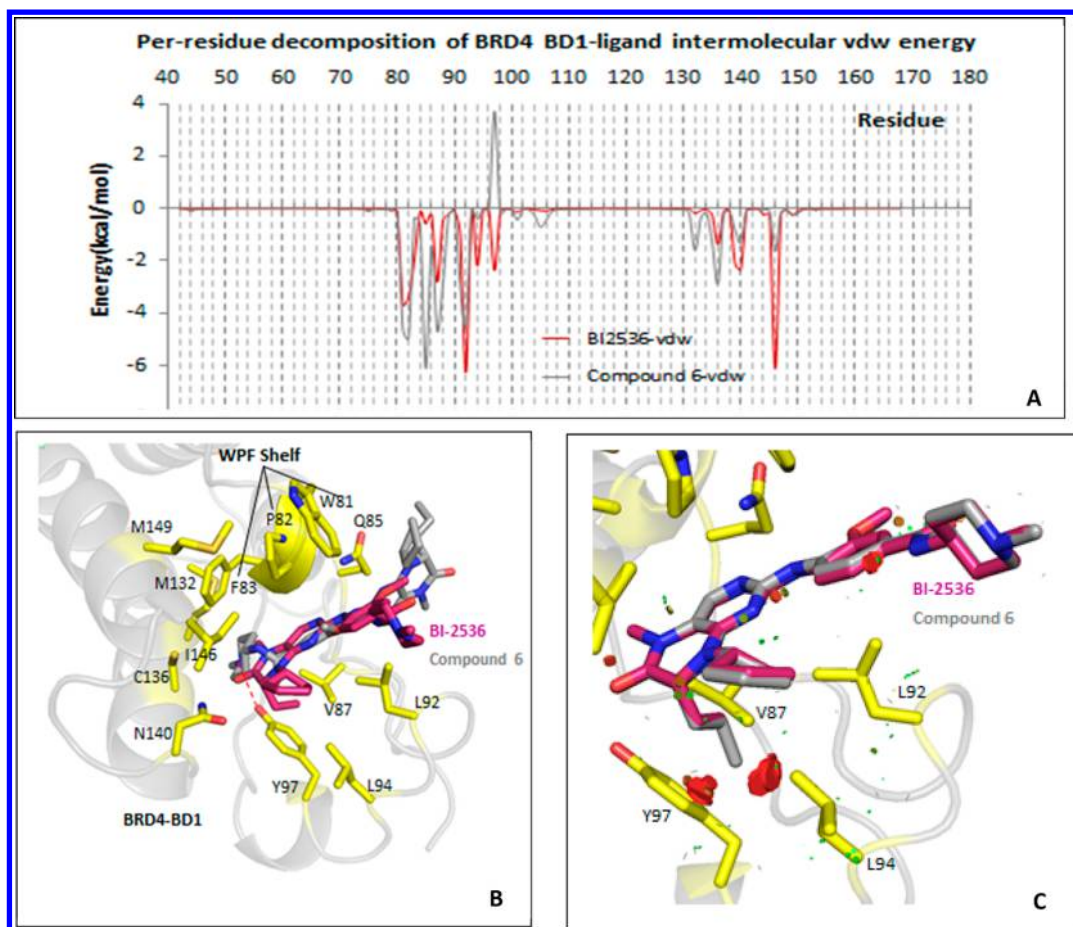


**Figure 6.** (A) Comparison of the per-residue decomposition of two BRD4-BD1 ligands, **6** in gray and BI-2536 in dark red, with intermolecular vdw interactions as a function of the receptor sequence. (B) Docking of **6** (gray) in BRD4 (1) (PDBID: 4O74); protein residues in contact with the ligand are represented by yellow sticks, and the rest are in gray. (C) Steric clashes caused by the propyl group if **6** is docked to BRD4 (1) in the same pose as BI-2536 (bumps are shown in red).

methyl group improved the inhibitory activity of the resulting compounds against both BRD4 and PLK1, as seen with compound **5**. Installing bulky alkyl groups at the asymmetric carbon resulted in inhibitors with potent and selective PLK1 activity but largely limited BRD4 activity, as seen with compound **6**. Further modification on the methoxy group of compound **5** led to the identification of compound **23**, a compound with increased potency for BRD4 and much reduced PLK1 activity. Our molecular docking studies suggested possible binding orientations with BRD4-BD1 and PLK1, and the binding energies were in agreement with the observed SAR established through our medicinal chemistry exercise.

In summary, we have demonstrated that fine-tuning the selectivity for inhibitors demonstrating polypharmacology can be achieved through structural guidance. We initiated an SAR campaign of BI-2536 in order to alter the PLK1 and BRD4 potency/selectivity of the compound and confirmed our biochemical findings through molecular modeling. In this study, we discovered a set of compounds with balanced selectivity against BRD4 and PLK1 that will entitle us to further explore the biological outcome of dual BRD4/PLK1 inhibition. In particular, compound **23** is a well-balanced BRD4 and PLK1 dual inhibitor when assayed biochemically and in cells. Compound **23** demonstrates an increased potency for BRD4 and a decreased potency for PLK1 as compared to

parent molecule BI-2536. We envision that this set of molecules will generate sufficient PLK1 and BRD4 inhibition in order to study the simultaneous targeting of PLK1 and BRD4 in cancer.

## EXPERIMENTAL SECTION

**General Synthetic Information.** All chemicals and solvents were purchased from commercial suppliers and used as received.  $^1\text{H}$  NMR (300 MHz) and  $^{13}\text{C}$  NMR (75 MHz) spectra were recorded on a Varian NMR spectrometer, and  $^1\text{H}$  NMR (400 MHz) and  $^{13}\text{C}$  NMR spectra (101 MHz) were recorded on Agilent NMR spectrometers. LCMS analyses were performed on an Agilent 2100 LC with a 6130 quadrupole MS spectrometer. Accurate mass measurements were performed on a Fusion Lumos Orbitrap mass spectrometer (Thermo Fisher Scientific) at a mass resolution setting of 500 000 immediately after calibration or under lock mass calibration using solvent ions. A  $\text{C}_{18}$  column (5.0  $\mu\text{m}$ , 6.0  $\times$  50  $\text{mm}^2$ ) was used for separation. The mobile phases were MeOH and  $\text{H}_2\text{O}$ , both containing 0.05%  $\text{CF}_3\text{CO}_2\text{H}$ . A linear gradient from 25/75 (v/v) MeOH/ $\text{H}_2\text{O}$  to 100% MeOH over 7.0 min at a flow rate of 0.7 mL/min was used as a mobile phase. UV detections were conducted at 210, 254, and 365 nm. Low-resolution mass spectra were recorded by APCI (atmospheric pressure chemical ionization) unless otherwise specified. Flash chromatography separation was performed on a YAMAZEN AI-580 system with Agela silica gel (12 or 20 g, 230–400 mesh) cartridges. Final products were purified on an Agela HP 100 preparative LC system with a Venusil PrepG  $\text{C}_{18}$  column (10  $\mu\text{m}$ ,

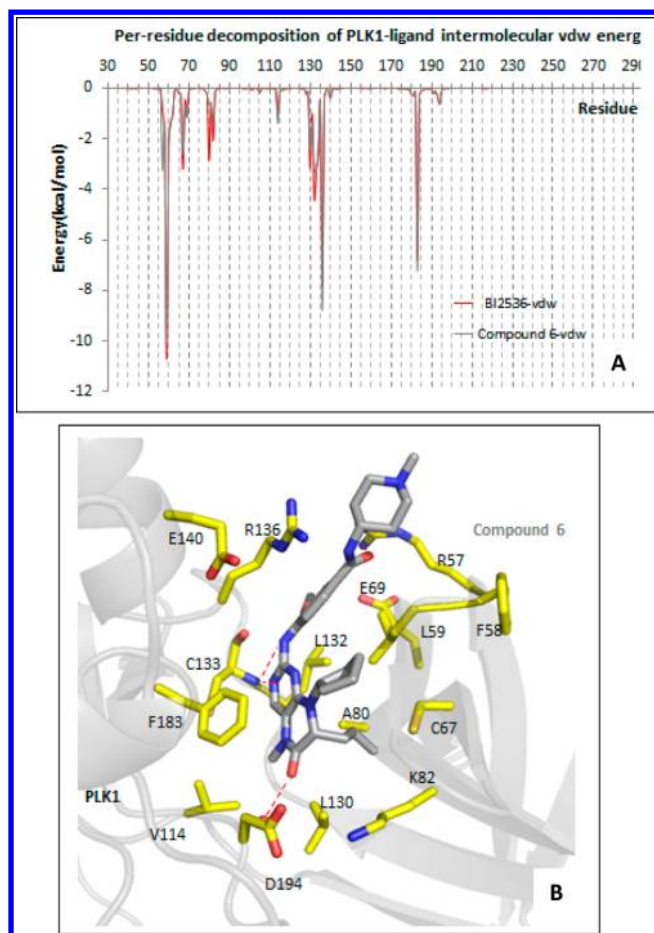


**Figure 7.** (A) Comparison of the per-residue decomposition of two PLK1-ligands, **6** in gray and BI-2536 in dark red, with intermolecular vdw interactions as a function of the receptor sequence. (B) Docking of **6** (gray) in PLK1 (PDBID: 2RKU); protein residues in contact with the ligand are represented by yellow sticks with the rest in gray, and hydrogen bonding is represented by red dashed lines.

120 Å,  $21.2 \times 250 \text{ mm}^2$ ). All biologically evaluated compounds were found to be >95% pure as determined by NMR and LCMS.

**Synthesis of BI-2536 Analogues.** The synthesis of compounds **1–20** shown in Tables 1 and 2 was carried out following the reported procedures (Scheme 1).<sup>34</sup> The synthesis of analogues of compound **5**, including compounds **21** and **23–25** listed in Table 2, was performed following the route shown in Scheme 2. Bromocyclopentane (1.3 equiv) was added slowly to a stirred suspension of potassium carbonate (1.5 equiv) in DMF containing methyl-3-hydroxy-4-nitrobenzoate (1 equiv) at 65 °C for 4 h, and then the product was treated by  $\text{SnCl}_2 \cdot 2\text{H}_2\text{O}$  in EtOAc at 50 °C overnight. A mixture of Ar-Cl (1 equiv), X-Phos (28 mol %),  $\text{Pd}_2(\text{dba})_3$  (7 mol %), methyl 4-amino-3-(cyclopentyloxy)benzoate (1.3 equiv), and  $\text{K}_2\text{CO}_3$  (5 equiv) in *t*-BuOH was heated at 100 °C in a sealed tube for 8 h. The mixture was then diluted with EtOAc and washed three times with aqueous  $\text{NaHCO}_3$ . The organic layer was dried over anhydrous  $\text{Na}_2\text{SO}_4$ , filtered, and condensed. The crude product was purified by a preparative LC system to obtain the final product.

(*R*)-4-((8-Cyclopentyl-5,7-dimethyl-6-oxo-5,6,7,8-tetrahydropteridin-2-yl)amino)-3-methoxy-*N*-(1-methylpiperidin-4-yl)benzamide (**5**).  $^1\text{H}$  NMR (300 MHz,  $\text{CD}_3\text{OD}$ )  $\delta$  8.41 (1H, d,  $J = 9.0$  Hz), 7.72 (1H, s), 7.41–7.31 (3H, m), 4.50–4.45 (1H, m), 4.31–4.24 (1H, q,  $J = 6.7$  Hz), 4.02–3.82 (6H, s,  $\text{N}-\text{CH}_3$  and  $\text{O}-\text{CH}_3$ ), 3.27–3.26 (6H, m), 3.22 (3H, s), 2.57–2.47 (6H, m), 2.06–1.86 (4H, m), 1.25 (3H, d,  $J = 6.6$  Hz);  $^{13}\text{C}$  NMR (75 MHz,  $\text{CD}_3\text{OD}$ )  $\delta$  170.9, 166.6, 156.3, 153.0, 139.44, 138.7, 127.3, 121.2, 117.3, 117.3, 109.9, 59.5, 59.3, 56.4, 55.6, 55.02, 47.1, 44.9, 31.2, 30.5, 29.9, 28.5, 24.3, 23.8, 19.0;

HRMS (ESI)  $m/z$ : ( $\text{M} + \text{H}$ )<sup>+</sup> calcd for  $\text{C}_{27}\text{H}_{37}\text{N}_7\text{O}_3$  536.3349, found 508.3031 ( $\text{M}^+ + 1$ ).

(*R*)-4-((8-Cyclopentyl-5-methyl-6-oxo-7-propyl-5,6,7,8-tetrahydropteridin-2-yl)amino)-3-methoxy-*N*-(1-methylpiperidin-4-yl)benzamide (**6**).  $^1\text{H}$  NMR (400 MHz,  $\text{CDCl}_3$ )  $\delta$  8.54 (1H, d,  $J = 8.4$  Hz), 7.68 (1H, s), 7.59 (1H, s), 7.51 (1H, s), 7.42 (1H, s), 7.42 (1H, d,  $J = 1.8$  Hz), 4.56–4.46 (1H, m), 4.24 (1H, dd,  $J = 8.0, 3.7$  Hz), 3.97 (3H, s), 3.31 (3H, s), 2.86–2.84 (2H, m), 2.31 (3H, s), 2.25–2.10 (4H, m), 2.07–2.04 (4H, m), 1.81–1.71 (14H, m), 1.37–1.21 (4H, m), 0.87 (3H, t,  $J = 7.3$  Hz);  $^{13}\text{C}$  NMR (101 MHz,  $\text{CDCl}_3$ )  $\delta$  163.9, 155.0, 152.1, 147.2, 137.9, 133.2, 126.2, 126.0, 118.8, 116.4, 115.8, 109.0, 58.8, 58.1, 54.4, 35.8, 32.4, 29.6, 29.1, 28.2, 23.5, 23.0, 17.8, 13.9; HRMS (ESI)  $m/z$ : ( $\text{M} + \text{H}$ )<sup>+</sup> calcd for  $\text{C}_{29}\text{H}_{41}\text{N}_7\text{O}_3$  536.3349, found 536.3342 ( $\text{M}^+ + 1$ ).

(*R*)-4-((8-Cyclopentyl-7-isobutyl-5-methyl-6-oxo-5,6,7,8-tetrahydropteridin-2-yl)amino)-3-methoxy-*N*-(1-methylpiperidin-4-yl)benzamide (**8**).  $^1\text{H}$  NMR (300 MHz,  $\text{CD}_3\text{OD}$ )  $\delta$  8.40 (1H, d,  $J = 9.0$  Hz), 7.74 (1H, s), 7.42–7.38 (3H, m), 4.21–4.17 (1H, m), 3.91 (3H, s), 3.87–3.83 (1H, m), 3.23 (3H, s), 2.91–2.88 (1H, m), 2.27 (3H, s), 2.21–2.13 (2H, m), 2.02–1.97 (2H, m), 1.92–1.83 (2H, m), 1.74–1.54 (8H, m), 1.41–1.36 (1H, m), 0.92 (3H, d,  $J = 6.3$  Hz), 0.78 (3H, d,  $J = 6.6$  Hz);  $^{13}\text{C}$  NMR (75 MHz,  $\text{CD}_3\text{OD}$ )  $\delta$  169.1, 165.2, 156.2, 153.6, 148.4, 139.6, 134.0, 127.4, 121.2, 117.4, 117.3, 109.9, 59.6, 58.4, 56.4, 55.5, 45.8, 42.5, 32.0, 30.49, 30.4, 28.6, 25.7, 24.2, 23.9, 23.7, 21.7; HRMS (ESI)  $m/z$ : ( $\text{M} + \text{H}$ )<sup>+</sup> calcd for  $\text{C}_{30}\text{H}_{43}\text{N}_7\text{O}_3$  550.3506, found 550.3501 ( $\text{M}^+ + 1$ ).

(*R*)-4-((8-Isopropyl-5,7-dimethyl-6-oxo-5,6,7,8-tetrahydropteridin-2-yl)amino)-3-methoxy-*N*-(1-methylpiperidin-4-yl)benzamide (**12**).  $^1\text{H}$  NMR (300 MHz,  $\text{CD}_3\text{OD}$ )  $\delta$  8.42 (1H, d,  $J = 9.3$  Hz), 7.69 (1H, s), 7.38 (3H, m), 3.99–3.90 (5H, m), 3.90 (3H, s), 2.72–2.65 (4H, m), 2.55 (3H, s), 1.86–1.76 (4H, m), 1.30–1.23 (9H, m);  $^{13}\text{C}$  NMR (75 MHz,  $\text{CD}_3\text{OD}$ )  $\delta$  169.2, 166.4, 156.3, 152.4, 148.3, 139.5, 134.1, 127.1, 121.3, 117.2, 109.8, 56.4, 54.7, 53.6, 46.6, 44.4, 30.7, 28.5, 21.5, 19.9; HRMS (ESI)  $m/z$ : ( $\text{M} + \text{H}$ )<sup>+</sup> calcd for  $\text{C}_{25}\text{H}_{35}\text{N}_7\text{O}_3$  482.2880, found 482.2884 ( $\text{M}^+ + 1$ ).

(*R*)-4-((8-Isobutyl-5-methyl-6-oxo-8-(tetrahydro-2H-pyran-4-yl)-5,6,7,8-tetrahydropteridin-2-yl)amino)-3-methoxy-*N*-(1-methylpiperidin-4-yl)benzamide (**13**).  $^1\text{H}$  NMR (300 MHz,  $\text{CD}_3\text{OD}$ )  $\delta$  8.42 (1H, d,  $J = 9.0$  Hz), 7.78 (1H, s), 7.45–7.42 (3H, m), 3.92 (3H, s), 3.56–3.53 (2H, m), 3.22 (3H, s), 3.03–2.99 (2H, m), 2.37 (3H, m), 1.96–1.92 (3H, m), 1.70–1.65 (4H, m), 1.55–1.38 (5H, m), 0.94 (3H, d,  $J = 6.3$  Hz), 0.79 (3H, d,  $J = 6.6$  Hz);  $^{13}\text{C}$  NMR (75 MHz,  $\text{CD}_3\text{OD}$ )  $\delta$  171.5, 171.4, 170.9, 169.1, 164.86, 153.0, 150.0, 140.1, 127.5, 121.2, 117.4, 110.0, 68.6, 68.5, 57.3, 56.4, 55.3, 55.2, 45.4, 43.4, 32.6, 31.6, 28.7, 25.8, 23.9, 21.7; HRMS (ESI)  $m/z$ : ( $\text{M} + \text{H}$ )<sup>+</sup> calcd for  $\text{C}_{30}\text{H}_{43}\text{N}_7\text{O}_4$  566.3455, found 566.3448 ( $\text{M}^+ + 1$ ).

(*S*)-4-((8-Cyclopentyl-5,7-dimethyl-6-oxo-5,6,7,8-tetrahydropteridin-2-yl)amino)-3-methoxy-*N*-(1-methylpiperidin-4-yl)benzamide (**21**).  $^1\text{H}$  NMR (300 MHz,  $\text{CD}_3\text{OD}$ )  $\delta$  8.43 (1H, d,  $J = 8.7$  Hz), 7.75 (1H, s), 7.43–7.41 (3H, m), 4.31–4.29 (1H, q,  $J = 6.0$  Hz), 3.94 (3H, s), 3.24 (3H, s), 3.12–3.07 (3H, m), 2.90–2.87 (3H, m), 2.12–2.09 (3H, m), 1.91–1.89 (4H, m), 1.79–1.67 (6H, m), 1.26 (3H, d,  $J = 6.9$  Hz);  $^{13}\text{C}$  NMR (75 MHz,  $\text{CD}_3\text{OD}$ )  $\delta$  171.1, 169.1, 166.6, 156.2, 153.0, 148.3, 139.4, 134.0, 127.4, 121.2, 117.2, 109.9, 59.3, 56.4, 55.6, 55.4, 47.8, 45.7, 31.9, 30.5, 29.9, 28.5, 24.2, 23.8, 19.0; HRMS (ESI)  $m/z$ : ( $\text{M} + \text{H}$ )<sup>+</sup> calcd for  $\text{C}_{31}\text{H}_{43}\text{N}_7\text{O}_3$  562.3506, found 562.3501 ( $\text{M}^+ + 1$ ).

(*R*)-4-((8-Cyclopentyl-5,7-dimethyl-6-oxo-5,6,7,8-tetrahydropteridin-2-yl)amino)-3-(cyclopentyloxy)-*N*-(1-methylpiperidin-4-yl)benzamide (**23**).  $^1\text{H}$  NMR (400 MHz,  $\text{CDCl}_3$ )  $\delta$  8.53 (1H, d,  $J = 8.0$  Hz), 7.71 (1H, s), 7.60 (1H, s), 7.41 (1H, d,  $J = 1.9$  Hz), 4.62–4.51 (1H, m), 4.32–4.30 (1H, m), 4.14–4.06 (1H, m), 3.97 (3H, s), 3.31 (3H, s), 2.83–2.81 (3H, m), 2.29 (3H, s), 2.20–2.10 (3H, m), 2.08–1.93 (4H, m), 1.32 (3H, d,  $J = 6.8$  Hz);  $^{13}\text{C}$  NMR (101 MHz,  $\text{CDCl}_3$ )  $\delta$  166.6, 165.0, 155.2, 151.8, 147.2, 138.3, 133.1, 126.6, 118.8, 116.3, 116.0, 109.1, 57.6, 55.9, 54.4, 46.2, 32.5, 30.0, 29.5, 28.3, 23.7, 23.2, 19.0. HRMS (ESI)  $m/z$ : ( $\text{M} + \text{H}$ )<sup>+</sup> calcd for  $\text{C}_{31}\text{H}_{43}\text{N}_7\text{O}_3$  562.3506, found 562.3508 ( $\text{M}^+ + 1$ ).

(*R*)-4-((8-Cyclopentyl-5-methyl-6-oxo-7-propyl-5,6,7,8-tetrahydropteridin-2-yl)amino)-3-(cyclopentyloxy)-*N*-(1-methylpiperidin-4-yl)benzamide (**24**).  $^1\text{H}$  NMR (300 MHz,  $\text{CD}_3\text{OD}$ )  $\delta$  8.44 (1H, d,  $J$

= 8.1 Hz), 7.72 (1H, s), 7.42–7.39 (3H, m), 4.39–4.34 (1H, m), 4.27–4.24 (1H, m), 3.85–3.80 (1H, m), 3.25 (3H, s), 2.86–2.60 (2H, m), 2.26 (3H, s), 2.16–2.09 (3H, m), 2.01–1.80 (14H, m), 1.76–1.59 (8H, m), 1.26–1.17 (2H, m), 0.83 (3H, t,  $J = 7.2$  Hz);  $^{13}\text{C}$  NMR (75 MHz,  $\text{CD}_3\text{OD}$ )  $\delta$  169.12, 165.4, 156.0, 153.4, 146.5, 139.0, 134.8, 127.3, 120.8, 117.2, 112.4, 81.8, 60.67, 60.5, 55.6, 49.7, 46.0, 36.8, 33.6, 32.2, 30.2, 29.9, 28.4, 24.8, 24.4, 24.2, 18.7, 14.0; HRMS (ESI)  $m/z$ : ( $\text{M} + \text{H}$ ) $^+$  calcd for  $\text{C}_{33}\text{H}_{47}\text{N}_7\text{O}_3$  590.3819, found 590.3815 ( $\text{M}^+ + 1$ ).

4-((8-Cyclopentyl-5-methyl-6-oxo-5,6,7,8-tetrahydropteridin-2-yl)amino)-3-(cyclopentyloxy)-*N*-(1-methylpiperidin-4-yl)benzamide (25).  $^1\text{H}$  NMR (300 MHz,  $\text{CD}_3\text{OD}$ )  $\delta$  8.43 (1H, d,  $J = 8.4$  Hz), 7.64 (1H, s), 7.42–7.39 (3H, m), 4.06 (3H, s), 3.28–3.25 (4H, m), 3.23 (3H, s), 3.02–2.97 (3H, m), 2.37 (3H, s), 2.30–2.26 (3H, m), 1.98–1.93 (7H, m), 1.74–1.68 (9H, m);  $^{13}\text{C}$  NMR (75 MHz,  $\text{CD}_3\text{OD}$ )  $\delta$  169.1, 163.5, 156.1, 153.1, 146.4, 138.5, 134.8, 127.1, 120.8, 117.0, 116.8, 112.3, 81.8, 56.9, 55.37, 47.6, 45.9, 45.5, 33.6, 31.7, 28.0, 27.9, 24.8, 24.8; HRMS (ESI)  $m/z$ : ( $\text{M} + \text{H}$ ) $^+$  calcd for  $\text{C}_{30}\text{H}_{41}\text{N}_7\text{O}_3$  548.3350, found 548.3346 ( $\text{M}^+ + 1$ ).

**Molecular Docking Software.** For protein preparation, UCSF Chimera Dock Prep tool<sup>35</sup> and UCSF DOCK6<sup>36</sup> were used. For compound structures and the charge assignment method, ChemDraw 15.0, Chem3D 14.0, GAFF, and AM1-BCC were used. For docking and energy decomposition analysis, the UCSF DOCK6 suite was used. For dock poses, visualization, and illustration, UCSF Chimera ViewDock and PyMOL were used.

**Compounds and Protein Preparation.** The synthesized compounds were built in ChemDraw, and then their Cartesian coordinates' construction and energy minimization using MM2 force field<sup>37,38</sup> were generated in Chem3D. The crystal structures of BI-2536 binding with BRD4-BD1 (PDBID: 4O74) and PLK1 (PDBID: 2RKU) were downloaded from the Protein Data Bank (PDB) archive. Protein targets were prepared using the Chimera DockPrep tool, in which AMBER force field ff14SB<sup>39</sup> was employed to provide accurate descriptions for proteins. GAFF<sup>40</sup> and AM1-BCC<sup>41</sup> were used to generate parameters and assign charges for all inhibitor molecules.

**Docking and Energy Decomposition Analysis.** The DOCK6 suite was used for docking compounds to their protein targets. Flexible ligand docking was performed under the guidance of Anchor-and-Grow algorithm. Dock Score was used as the criterion for ranking the binding poses. We visually examined the top 10 ranked poses, and the highest ranked poses are reported in Table 3. In the case of PLK1 and BRD4-BD1, DOCK6 successfully sampled and top-scored the BI-2536 docking poses to reproduce the corresponding crystal binding poses with an rmsd < 2 Å. DOCK Score is composed of van der Waals (vdw) and electrostatic interactions. The vdw composition of Dock Score was further decomposed onto every residue of its binder protein by using DOCK write\_footprint function, which generates both the vdw and electrostatic parts. Only the vdw composition was noticeably diversified and thus referred to represent the contribution of the protein target per residue in protein–ligand interaction energy profiles as shown in Figures 4–7.

**Specific Favorable and Unfavorable Interactions Recognition.** As listed in Table 3, the specific residual information of the protein receptors interacting with BI-2536 analogues was recognized by referring to vdw energy and by the visualization of binding poses. A threshold of < –4 kcal/mol in decomposed vdw energy was used to include the first shell of residues around the molecules (also see Supporting Information Figure S-3). The positive peak observed in the per-residue decomposition of BRD4-BD1 compound 6, Figure 6A, was ascribed to the steric clashes of residues Y97, L94 with the propyl group on 6. The disc was scripted in PyMOL software to show vdw overlaps or steric clashing (also see Supporting Information Figure S-4).

**BRD4-BD1 and BRDT-BD1 Activity Assays.** Compound potency was assessed by relative  $\text{IC}_{50}$  potency determined by an AlphaScreen biotin–JQ1 competition assay as reported previously by our group.<sup>42</sup> All reagents were diluted in 50 mM HEPES, 150 mM NaCl, 0.1% w/v BSA, and 0.01% w/v Tween20, pH 7.5, and allowed to equilibrate to room temperature prior to the addition to plates.

After the addition of Alpha beads to the master solutions, all subsequent steps were performed in low-light conditions. A 2× solution of components with final concentrations of BRD at 40 nM, Ni-coated acceptor bead at 25  $\mu\text{g/mL}$ , and 20 nM biotin–JQ1 was added in 10  $\mu\text{L}$  to 384-well plates (AlphaPlate-384, PerkinElmer, USA). After a 1 min 1000 rpm spin down, 100 nL portions of compounds in DMSO from stock plates were added by pin transfer using a Janus Workstation (PerkinElmer, USA). The 2×, 10  $\mu\text{L}$  of streptavidin-coated donor beads (25  $\mu\text{g/mL}$ ) were added to the previous solution. Following this addition, the plates were sealed with foil to block light exposure and to prevent evaporation. The plates were spun down again at 1000 rpm for 1 min. Next, the plates were incubated at room temperature with the plate reader (for temperature equilibration) for 1 h prior to reading the assay. The signal is stable for up to 3 h after donor bead addition. AlphaScreen measurements were performed on an Envision 2104 (PerkinElmer, USA) utilizing the manufacturer's protocol.

**PLK1 Activity Assay.** The enzymatic activities against PLK1 were tested in Z-Lyte assays with an ATP concentration of  $K_M$  for each kinase per manufacturer's protocol (Thermo Fisher).

All the compounds were tested in parallel with the cross-linker assay to rule out the assay binder/interrupter.

**Selectivity Profiling.** Compound 5 was assayed at 1  $\mu\text{M}$  in DiscoverX's BROMOscan (bromoMAX) and KINOMEScan (scan-MAX) assay platforms. The results for single-concentration binding interactions for compound 5 are reported as the % of control (DMSO).

**Cell Cycle Study.** MOLM13 cells were treated with 1  $\mu\text{M}$  JQ1, BI2536, TAE684, compound 5, compound 6, or compound 23 for 24 h. Cells were subsequently harvested and stained with propidium iodide (Calbiochem); this was followed by the measurement of propidium-iodide-mediated fluorescence with a Guava H6T (Millipore Sigma).

## ■ ASSOCIATED CONTENT

### ● Supporting Information

The Supporting Information is available free of charge on the ACS Publications website at DOI: 10.1021/acs.jmedchem.8b00765.

BROMOscan and KINOMEScan data for 5 (PDF)

Molecular formula strings (CSV)

### Accession Codes

PDB codes are the following: 4O74 for BI2536, BRD4-BD1; 2RKU for PLK1-BI2536.

## ■ AUTHOR INFORMATION

### Corresponding Authors

\*E-mail: james.bradner@novartis.com. Tel: +1 (617) 871-8000. Fax: +1 (617) 582-7370.

\*E-mail: jun\_qi@dfci.harvard.edu. Tel: +1 (617) 632-6629. Fax: +1 (617) 582-7370.

\*E-mail: wei2.zhang@umb.edu. Tel: +1 (617) 287-6147. Fax: +1 (617) 287-6030.

### ORCID

James E. Bradner: 0000-0002-2718-4415

Jun Qi: 0000-0002-1461-3356

Wei Zhang: 0000-0002-6097-2763

### Author Contributions

All authors have given approval to the final version of the manuscript.

### Notes

The authors declare no competing financial interest.

## ■ ACKNOWLEDGMENTS

This work was partially supported by National Institutes of Health U54 grant CA156732 (J.E.B. and W.Z.), U54 grant (HD093540-01 for J.Q.), and P01 grant (CA066996 for J.Q.). We thank Jason Evans and Dennis Zeh for performing the HRMS analysis of some synthetic compounds.

## ■ ABBREVIATIONS USED

BET, bromodomain and extra-terminal domain; BRD4, bromodomain 4; PLK1, polo-like kinase; AML, acute myeloid leukemia; JAK2, janus kinase 2; SAR, structure–activity relationship; LID, ligand interaction diagrams

## ■ REFERENCES

- (1) Wang, C. Y.; Filippakopoulos, P. Beating the odds: BETs in disease. *Trends Biochem. Sci.* **2015**, *40*, 468–479.
- (2) Boehm, D.; Calvanese, V.; Dar, R. D.; Xing, S.; Schroeder, S.; Martins, L.; Aull, K.; Li, P. C.; Planelles, V.; Bradner, J. E.; Zhou, M. M.; Siliciano, R. F.; Weinberger, L.; Verdin, E.; Ott, M. BET bromodomain-targeting compounds reactivate HIV from latency via a Tat-independent mechanism. *Cell Cycle* **2013**, *12*, 452–462.
- (3) Delmore, J. E.; Issa, G. C.; Lemieux, M. E.; Rahl, P. B.; Shi, J.; Jacobs, H. M.; Kastritis, E.; Gilpatrick, T.; Paranal, R. M.; Qi, J.; Chesi, M.; Schinzel, A. C.; McKeown, M. R.; Heffernan, T. P.; Vakoc, C. R.; Bergsagel, P. L.; Ghobrial, I. M.; Richardson, P. G.; Young, R. A.; Hahn, W. C.; Anderson, K. C.; Kung, A. L.; Bradner, J. E.; Mitsiades, C. S. BET bromodomain inhibition as a therapeutic strategy to target c-Myc. *Cell* **2011**, *146*, 904–917.
- (4) Bandukwala, H. S.; Gagnon, J.; Togher, S.; Greenbaum, J. A.; Lamperti, E. D.; Parr, N. J.; Molesworth, A. M.; Smithers, N.; Lee, K.; Witherington, J.; Tough, D. F.; Prinjha, R. K.; Peters, B.; Rao, A. Selective inhibition of CD4+ T-cell cytokine production and autoimmunity by BET protein and c-Myc inhibitors. *Proc. Natl. Acad. Sci. U. S. A.* **2012**, *109*, 14532–14537.
- (5) Gallenkamp, D.; Gelato, K. A.; Haendler, B.; Weinmann, H. Bromodomains and their pharmacological inhibitors. *ChemMedChem* **2014**, *9*, 438–464.
- (6) Filippakopoulos, P.; Knapp, S. Targeting bromodomains: epigenetic readers of lysine acetylation. *Nat. Rev. Drug Discovery* **2014**, *13*, 337–356.
- (7) Prinjha, R. K.; Witherington, J.; Lee, K. Place your BETs: the therapeutic potential of bromodomains. *Trends Pharmacol. Sci.* **2012**, *33*, 146–153.
- (8) Vidler, L. R.; Brown, N.; Knapp, S.; Hoelder, S. Druggability analysis and structural classification of bromodomain acetyl-lysine binding Sites. *J. Med. Chem.* **2012**, *55*, 7346–7359.
- (9) Filippakopoulos, P.; Knapp, S. The bromodomain interaction module. *FEBS Lett.* **2012**, *586*, 2692–2704.
- (10) Hewings, D. S.; Rooney, T. P.; Jennings, L. E.; Hay, D. A.; Schofield, C. J.; Brennan, P. E.; Knapp, S.; Conway, S. J. Progress in the development and application of small molecule inhibitors of bromodomain–acetyl lysine interactions. *J. Med. Chem.* **2012**, *55*, 9393–9413.
- (11) Chung, C. W. Small molecule bromodomain inhibitors: extending the druggable genome. *Prog. Med. Chem.* **2012**, *51*, 1–55.
- (12) Yang, Z.; Yik, J. H.; Chen, R.; He, N.; Jang, M. K.; Ozato, K.; Zhou, Q. Recruitment of P-TEFb for stimulation of transcriptional elongation by the bromodomain protein Brd4. *Mol. Cell* **2005**, *19*, 535–545.
- (13) Jang, M. K.; Mochizuki, K.; Zhou, M.; Jeong, H. S.; Brady, J. N.; Ozato, K. The bromodomain protein Brd4 is a positive regulatory component of P-TEFb and stimulates RNA polymerase II-dependent transcription. *Mol. Cell* **2005**, *19*, 523–534.
- (14) Filippakopoulos, P.; Qi, J.; Picaud, S.; Shen, Y.; Smith, W. B.; Fedorov, O.; Morse, E. M.; Keates, T.; Hickman, T. T.; Felletar, I.; Philpott, M.; Munro, S.; McKeown, M. R.; Wang, Y.; Christie, A. L.; West, N.; Cameron, M. J.; Schwartz, B.; Heightman, T. D.; La Thangue, N.; French, C. A.; Wiest, O.; Kung, A. L.; Knapp, S.; Bradner, J. E. Selective inhibition of BET bromodomains. *Nature* **2010**, *468*, 1067–1073.
- (15) Nicodeme, E.; Jeffrey, K. L.; Schaefer, U.; Beinke, S.; Dewell, S.; Chung, C. W.; Chandwani, R.; Marazzi, I.; Wilson, P.; Coste, H.; White, J.; Kirilovsky, J.; Rice, C. M.; Lora, J. M.; Prinjha, R. K.; Lee, K.; Tarakhovsky, A. Suppression of inflammation by a synthetic histone mimic. *Nature* **2010**, *468*, 1119–1123.
- (16) Mirguet, O.; Lamotte, Y.; Donche, F.; Toum, J.; Gellibert, F.; Bouillot, A.; Gosmini, R.; Nguyen, V. L.; Delannee, D.; Seal, J.; Blandel, F.; Boullay, A. B.; Boursier, E.; Martin, S.; Brusq, J. M.; Krysa, G.; Riou, A.; Tellier, R.; Costaz, A.; Huet, P.; Dudit, Y.; Trotter, L.; Kirilovsky, J.; Nicodeme, E. From ApoA1 upregulation to BET family bromodomain inhibition: Discovery of I-BET151. *Bioorg. Med. Chem. Lett.* **2012**, *22*, 2963–2967.
- (17) Fish, P. V.; Filippakopoulos, P.; Bish, G.; Brennan, P. E.; Bunnage, M. E.; Cook, A. S.; Federov, O.; Gerstenberger, B. S.; Jones, H.; Knapp, S.; Marsden, B.; Nocka, K.; Owen, D. R.; Philpott, M.; Picaud, S.; Primiano, M. J.; Ralph, M. J.; Sciammetta, N.; Trzupke, J. D. Identification of a chemical probe for bromo and extra C-terminal bromodomain inhibition through optimization of a fragment-derived hit. *J. Med. Chem.* **2012**, *55*, 9831–9837.
- (18) Tanaka, M.; Roberts, J. M.; Qi, J.; Bradner, J. E. Inhibitors of emerging epigenetic targets for cancer therapy: A patent review (2010–2014). *Pharm. Pat. Anal.* **2015**, *4*, 261–284.
- (19) Garnier, J. M.; Sharp, P. P.; Burns, C. J. BET bromodomain inhibitors: a patent review. *Expert Opin. Ther. Pat.* **2014**, *24*, 185–199.
- (20) Sanchez, R.; Meslamani, J.; Zhou, M. M. The bromodomain: from epigenome reader to druggable target. *Biochim. Biophys. Acta, Gene Regul. Mech.* **2014**, *1839*, 676–685.
- (21) Shortt, J.; Ott, C. J.; Johnstone, R. W.; Bradner, J. E. A chemical probe toolbox for dissecting the cancer epigenome. *Nat. Rev. Cancer* **2017**, *17*, 160–183.
- (22) Shu, S.; Lin, C. Y.; He, H. H.; Witwicki, R. M.; Tabassum, D. P.; Roberts, J. M.; Janiszewska, M.; Huh, S. J.; Liang, Y.; Ryan, J.; Doherty, E.; Mohammed, H.; Guo, H.; Stover, D. G.; Ekram, M. B.; Brown, J.; D'Santos, C.; Krop, I. E.; Dillon, D.; McKeown, M.; Ott, C.; Qi, J.; Ni, M.; Rao, P. K.; Duarte, M.; Wu, S. Y.; Chiang, C. M.; Anders, L.; Young, R. A.; Winer, E.; Letai, A.; Barry, W. T.; Carroll, J. S.; Long, H.; Brown, M.; Liu, X. S.; Meyer, C. A.; Bradner, J. E.; Polyak, K. Response and resistance to BET bromodomain inhibitors in triple-negative breast cancer. *Nature* **2016**, *529*, 413–417.
- (23) Gutteridge, R. E.; Ndiaye, M. A.; Liu, X.; Ahmad, N. PLK1 inhibitors in cancer therapy: From laboratory to clinics. *Mol. Cancer Ther.* **2016**, *15*, 1427–1435.
- (24) Seton-Rogers, S. Epigenetics: Place your BETs. *Nat. Rev. Cancer* **2015**, *15*, 638.
- (25) Mao, F.; Li, J.; Luo, Q.; Wang, R.; Kong, Y.; Carlock, C.; Liu, Z.; Elzey, B. D.; Liu, X. PLK1 inhibition enhances the efficacy of bet epigenetic reader blockade in castration-resistant prostate cancer. *Mol. Cancer Ther.* **2018**, *17*, 1554–1565.
- (26) Tontsch-Grunt, U.; Rudolph, D.; Waizenegger, I.; Baum, A.; Gerlach, D.; Engelhardt, H.; Wurm, M.; Savarese, F.; Schweifer, N.; Kraut, N. Synergistic activity of BET inhibitor BI 894999 with PLK inhibitor volasertib in AML in vitro and in vivo. *Cancer Lett.* **2018**, *421*, 112–120.
- (27) Andrews, F. H.; Singh, A. R.; Joshi, S.; Smith, C. A.; Morales, G. A.; Garlich, J. R.; Durden, D. L.; Kutateladze, T. G. Dual-activity PI3K–BRD4 inhibitor for the orthogonal inhibition of MYC to block tumor growth and metastasis. *Proc. Natl. Acad. Sci. U. S. A.* **2017**, *114*, E1072–E1080.
- (28) Singh, A. R.; Joshi, S.; Burgoyne, A. M.; Sicklick, J. K.; Ikeda, S.; Kono, Y.; Garlich, J. R.; Morales, G. A.; Durden, D. L. Single agent and synergistic activity of the “first-in-class” Dual PI3K/BRD4 inhibitor SF1126 with sorafenib in hepatocellular carcinoma. *Mol. Cancer Ther.* **2016**, *15*, 2553–2562.
- (29) Ember, S. W.; Zhu, J. Y.; Olesen, S. H.; Martin, M. P.; Becker, A.; Berndt, N.; Georg, G. I.; Schonbrunn, E. Acetyl-lysine binding site

of bromodomain-containing protein 4(BRD4) interacts with diverse kinase inhibitors. *ACS Chem. Biol.* **2014**, *9*, 1160–1171.

(30) Ciceri, P.; Muller, S.; O'Mahony, A. Dual kinase-bromodomain inhibitors for rationally designed polypharmacology. *Nat. Chem. Biol.* **2014**, *10*, 305–312.

(31) Koblan, L. W.; Buckley, D. L.; Ott, C. J.; Fitzgerald, M. E.; Ember, S. W.; Zhu, J. Y.; Liu, S.; Roberts, J. M.; Remillard, D.; Vittori, S.; Zhang, W.; Schonbrunn, E.; Bradner, J. E. Assessment of bromodomain target engagement by a series of BI2536 analogues with miniaturized BET-BRET. *ChemMedChem* **2016**, *11*, 2575–2581.

(32) Chen, L.; Yap, J. L.; Yoshioka, M.; Lanning, M. E.; Fountain, R. N.; Raje, M.; Scheenstra, J. A.; Strovel, J. W.; Fletcher, S. BRD4 structure–activity relationships of dual PLK1 Kinase/BRD4 bromodomain inhibitor BI-2536. *ACS Med. Chem. Lett.* **2015**, *6*, 764–769.

(33) Fabian, M. A.; Biggs, W. H., 3rd; Treiber, D. K.; Atteridge, C. E.; Azimioara, M. D.; Benedetti, M. G.; Carter, T. A.; Ciceri, P.; Edeen, P. T.; Floyd, M.; Ford, J. M.; Galvin, M.; Gerlach, J. L.; Grotzfeld, R. M.; Herrgard, S.; Insko, D. E.; Insko, M. A.; Lai, A. G.; Lelias, J. M.; Mehta, S. A.; Milanov, Z. V.; Velasco, A. M.; Wodicka, L. M.; Patel, H. K.; Zarrinkar, P. P.; Lockhart, D. J. A small molecule-kinase interaction map for clinical kinase inhibitors. *Nat. Biotechnol.* **2005**, *23*, 329–336.

(34) Zhang, Z.; Kwiatkowski, N.; Zeng, H.; Lim, S. M.; Gray, N. S.; Zhang, W.; Yang, P. L. Leveraging kinase inhibitors to develop small molecule tools for imaging kinases by fluorescence microscopy. *Mol. Biosyst.* **2012**, *8*, 2523–2526.

(35) Pettersen, E. F.; Goddard, T. D.; Huang, C. C.; Couch, G. S.; Greenblatt, D. M.; Meng, E. C.; Ferrin, T. E. UCSF Chimera - A visualization system for exploratory research and analysis. *J. Comput. Chem.* **2004**, *25*, 1605–1612.

(36) Allen, W. J.; Balias, T. E.; Mukherjee, S.; Brozell, S. R.; Moustakas, D. T.; Lang, P. T.; Case, D. A.; Kuntz, I. D.; Rizzo, R. C. DOCK 6: Impact of new features and current docking performance. *J. Comput. Chem.* **2015**, *36*, 1132–1156.

(37) Allinger, N. L. Conformational analysis. 130. MM2. A hydrocarbon force field utilizing V1 and V2 torsional terms. *J. Am. Chem. Soc.* **1977**, *99*, 8127–8134.

(38) Ponder, J. W.; Richards, F. M. An efficient newton-like method for molecular mechanics energy minimization of large molecules. *J. Comput. Chem.* **1987**, *8*, 1016–1024.

(39) Maier, J. A.; Martinez, C.; Kasavajhala, K.; Wickstrom, L.; Hauser, K. E.; Simmerling, C. ff14SB: Improving the accuracy of protein side chain and backbone parameters from FF99SB. *J. Chem. Theory Comput.* **2015**, *11*, 3696–3713.

(40) Wang, J.; Wolf, R. M.; Caldwell, J. W.; Kollman, P. A.; Case, D. A. Development and testing of a general amber force field. *J. Comput. Chem.* **2004**, *25*, 1157–1174.

(41) Jakalian, A.; Jack, D. B.; Bayly, C. I. Fast, efficient generation of high-quality atomic charges. AM1-BCC model: II. Parameterization and validation. *J. Comput. Chem.* **2002**, *23*, 1623–1641.

(42) McKeown, M. R.; Shaw, D. L.; Fu, H.; Liu, S.; Xu, X.; Marineau, J. J.; Huang, Y.; Zhang, X.; Buckley, D. L.; Kadam, A.; Zhang, Z.; Blacklow, S. C.; Qi, J.; Zhang, W.; Bradner, J. E. Biased multicomponent reactions to develop novel bromodomain inhibitors. *J. Med. Chem.* **2014**, *57*, 9019–9027.